We predicted and discovered (using the same data) local space volumes in which Einstein's antigravity due to dark energy is stronger than Newton's gravity from dark energy and baryons; the nearest such region is located at a distance of 1–3 Mpc from the Milky Way.

A new type of cosmic motion — local recession flows accelerated by dark energy — has been discovered in the antigravity regions.

The local dark energy density measured in these volumes turned out to be equal (within measurement errors) to the global dark energy density. This provides a new independent empirical argument in favor of Einstein's antigravity as a universal phenomenon, in the same sense as Newton's gravity is universal. This result is in contradiction with theories of modified gravity, which treat dark energy as an effect that is possible only at large distances.

The author thanks G G Byrd, G S Bisnovaty-Kogan, M U Valtonen, L M Domozhilova, A E Kantor, I D Karachentsev, D I Makarov, O G Nasonova, P Nurmi, P Teerikorpi, and P Heinämäki for their collaboration, as well as N V Emelyanov, Yu N Efremov, A V Zasov, and A M Cherepashchuk for the useful discussions.

References

1. Riess A G et al. *Astron. J.* **116** 1009 (1998)
2. Perlmutter S et al. *Astrophys. J.* **517** 565 (1999)
3. Einstein A *Sitzungsber. Königl. Preuß. Akad. Wissenschaft.* 142 (1917)
4. Hinshaw G et al., arXiv:1212.5226
5. Gliner E B *Sov. Phys. JETP* **22** 378 (1966) [*Zh. Eksp. Teor. Fiz.* **49** 542 (1965)]
6. Gliner É B *Sov. Phys. Dokl.* **15** 559 (1970) [*Dokl. Akad. Nauk SSSR* **192** 771 (1970)]
7. Gliner É B, Dymnikova I G *Sov. Astron. Lett.* **1** 93 (1975) [*Pis'ma Astron. Zh.* **1** (5) 7 (1975)]
8. Gliner E B *Phys. Usp.* **45** 213 (2002) [*Usp. Fiz. Nauk* **172** 221 (2002)]
9. Chernin A, Teerikorpi P, Baryshev Yu *Adv. Space Res.* **31** 459 (2003); astro-ph/0012021
10. Chernin A D *Phys. Usp.* **44** 1099 (2001) [*Usp. Fiz. Nauk* **171** 1153 (2001)]
11. Karachentsev I D et al. *Mon. Not. R. Astron. Soc.* **393** 1265 (2009)
12. Baryshev Yu V, Chernin A D, Teerikorpi P *Astron. Astrophys.* **378** 729 (2001)
13. Chernin A D et al. *Astron. Astrophys.* **415** 19 (2004)
14. Karachentsev I D *Astron. J.* **129** 178 (2005)
15. Karachentsev I D et al. *Astron. Astrophys.* **398** 479 (2003)
16. Karachentsev I D, Kashibadze O G *Astrophysics* **49** 3 (2006) [*Astrofizika* **49** 5 (2006)]
17. Karachentsev I D, Karachentseva V E, Huchtmeier W K *Astron. Lett.* **33** 512 (2007) [*Pis'va Astron. Zh.* **33** 577 (2007)]
18. Karachentsev I D et al. *Astron. J.* **131** 1361 (2006)
19. Chernin A D et al. *Astron. Astrophys.* **467** 933 (2007)
20. Chernin A D et al. *Astrophys.* **50** 405 (2007) [*Astrofizika* **50** 493 (2007)]
21. Chernin A D et al. *Astron. Astrophys. Trans.* **26** 275 (2007)
22. Karachentsev I D, Nasonova O G *Mon. Not. R. Astron. Soc.* **405** 1075 (2010)
23. Nasonova O G, de Freitas Pacheco J A, Karachentsev I D *Astron. Astrophys.* **532** 104 (2011)
24. Chernin A D et al. *Astron. Astrophys.* **520** 104 (2010)
25. Chernin A D et al. *Astron. Rep.* **56** 653 (2012) [*Astron. Zh.* **89** 723 (2012)]
26. Bisnovatyi-Kogan G S, Chernin A D *Astrophys. Space Sci.* **338** 337 (2012)
27. Chernin A D et al. *Astron. Astrophys.* **539** 4 (2012)
28. Chernin A D et al. *Astron. Astrophys.* **553** 101 (2013)
29. Teerikorpi P, Chernin A D *Astron. Astrophys.* **516** A93 (2010)
30. Chernin A D et al. *Astron. Astrophys.* **507** 1271 (2009)
31. Teerikorpi P et al. *Astron. Astrophys.* **483** 383 (2008)
32. Nurmi P, Heinämäki P, Teerikorpi P, Chernin A D *AIP Conf. Proc.* **1240** 419 (2010)
33. Byrd G G, Chernin A D, Teerikorpi P, Valtonen M *Paths to Dark Energy: Theory and Observation* (De Gruyter Studies in Mathematical Physics, 2) (Berlin: De Gruyter, 2012)
34. Byrd G et al. *Astron. J.* **107** 2055 (1994)
35. Chernin A D et al. *Astron. Astrophys.* **467** 933 (2007)
36. Chernin A D et al. *Astron. Astrophys.* **415** 19 (2004)
37. Chernin A D, Teerikorpi P, Baryshev Yu V *Astron. Astrophys.* **456** 13 (2006)
38. Teerikorpi P, Chernin A D, Baryshev Yu V *Astron. Astrophys.* **440** 791 (2005)
39. Karachentsev I D, Chernin A D, Teerikorpi P *Astrophysics* **46** 399 (2003) [*Astrofizika* **46** 491 (2003)]
40. Sandage A *Astrophys. J.* **527** 479 (1999)
41. Sandage A et al. *Astrophys. J.* **653** 843 (2006)

PACS numbers: **04.70.–s**, 97.60.Lf, 98.62.Js
DOI: 10.3367/UFNe.0183.201307f.0747

Investigating supermassive black holes: a new method based on the polarimetric observations of active galactic nuclei

Yu N Gnedin

1. Introduction

Presently, the existence of supermassive black holes (SMBHs) in active galactic nuclei (AGNs) is widely recognized. Rotating supermassive black holes are powerful engines responsible for energetic physical processes operating on a giant scale of the order of $10^{22}-10^{25}$ cm in galaxies. The characteristic phenomena related to SMBHs include radiation from the narrow emission line region ($\sim 10^{20}-10^{22}$ cm), broad emission line region ($\sim 10^{18}-10^{21}$ cm), region of nonthermal radiation ($\sim 10^{18}-10^{19}$ cm), and rapid X-ray variability region ($\sim 10^{13}$ cm). It is the central black hole that generates radiation in these space regions.

Active galactic nuclei hosting such SMBHs form a sufficiently homogeneous class of astronomical objects. The brightest AGNs have the bolometric luminosity $L_{\text{bol}} > 10^{47}$ erg s^{-1} and their masses can be as high as $\sim 10^{10} M_{\odot}$. Many AGNs demonstrate highly collimated outflows (jets) of matter moving with relativistic velocities normal to the disk. The size of the jets reach several dozen kiloparsecs, which exceeds the size of a galaxy.

Black holes are predicted by Einstein's General Relativity (GR). By definition, a black hole is a region of space from which no signal can escape. In other words, the escape velocity for a black hole is equal to the speed of light in the vacuum. The boundary of such a region is called the event horizon, R_{h}.

The characteristic size of a black hole is determined by the gravitational radius

$$R_{\text{g}} = \frac{GM}{c^2} \,,$$

Yu N Gnedin Main (Pulkovo) Astronomical Observatory
Russian Academy of Sciences, St. Petersburg, Russian Federation
E-mail: gnedin@gao.spb.ru

Uspekhi Fizicheskikh Nauk **183** (7) 747 – 752 (2013)
DOI: 10.3367/UFNr.0183.201307f.0747
Translated by K A Postnov; edited by A M Semikhatov

where M is the black hole mass, c is the speed of light, and G is Newton's gravitational constant. For a nonrotating, or Schwarzschild, black hole, the event horizon is $R_{\mathrm{h}} = 2R_{\mathrm{g}}$. For a rotating black hole,

$$R_{\mathrm{h}} = R_{\mathrm{g}}\left(1 + \sqrt{1 - a^2}\right),$$

where a is the dimensionless angular momentum usually called spin, $-1 \leqslant a \leqslant 1$. Negative spins correspond to the case where the sense of proper rotation of the black hole is opposite to that of the Keplerian motion of gas in the accretion disk (the so-called retrograde black hole rotation). For an extreme Kerr black hole with the maximum specific angular momentum, $R_{\mathrm{h}} = R_{\mathrm{g}}$. The radius of the last marginally stable orbit in which matter is captured by the black hole depends on the black-hole angular momentum and decreases for rotating black holes. For a nonrotating Schwarzschild black hole, $R_{\mathrm{st}} = 6R_{\mathrm{g}}$, and for an extreme Kerr black hole with the maximum angular momentum characterized by the spin $a_* = 0.998$, the last marginally stable orbit has $R_{\mathrm{h}} = 1.22R_{\mathrm{g}}$.

The AGN activity is explained by the accretion of matter onto the central supermassive black hole. A detailed theory of accretion flows has been elaborated starting from the 1940–1960s. The theory was especially strongly developed in the 1970s, when X-ray sources due to accretion onto neutron stars and black holes were discovered. The first simplest adiabatic (including spherically symmetric) accretion models were very helpful in understanding many features of real astrophysical objects. However, these models often did not explain the observed phenomena even qualitatively. In particular, radiation of gas during adiabatic accretion turned out to be too faint. The solution to this problem was found in the model of disk accretion, where nonadiabaticity effects necessarily become dominant.

The theory of hydrodynamic disk accretion has been developed since the late 1960s. However, many details remain unclear. Therefore, simplified models, such as the standard Shakura–Sunyaev disk accretion theory or the ADAF (advection-dominated accretion flow) theory are usually considered. In particular, a successful purely hydrodynamic model of the central engine in AGNs, which would reproduce effective matter outflows (jets) carrying away a significant fraction of the energy released, has not been constructed so far.

Currently, both the mechanism of energy generation that effectively transfers energy from the rotating black hole to active regions and the mechanism of matter outflow collimation are thought to be related to the regular poloidal magnetic field. Because black holes cannot have a proper magnetic field (the so-called "no-hair theorem"), the generation of a large-scale magnetic field near a black hole can occur in the accretion disk and in the region between the last marginally stable orbit and the black-hole horizon (the so-called plunge region). Ever-increasing computer power now allows constructing MHD models of accretion disks, a rapidly growing field of research. Some of these models are reviewed in [1]. However, so far, no direct evidence has been obtained of the existence of strong, dynamically significant magnetic fields in AGNs. Nevertheless, the presence of magnetic fields in AGNs is now paradigmatically recognized.

Therefore, measuring magnetic fields in accretion disks of AGNs is essential to understand their physical properties and energy generation mechanisms.

Spectropolarimetry is an effective method of studying basic structural components in quasars and AGNs, including the accretion disk, the broad emission line region, and the hot corona around the accretion disk. For many objects, emission from these regions is polarized. Polarization is due to scattering on plasma electrons, which are distributed anisotropically around the central black hole. The accretion disk is a typical example of an emission region with non-spherically symmetric electron density distribution. The broad emission line region also has a flat geometry.

The analysis of spectropolarimetric observations allows indirectly estimating the magnetic field strength using a method suggested in [2–4]. The method is based on the idea that if the Faraday rotation effect is taken into account in the process of electron scattering, then the degree and positional angle of polarization, as well as their dependence on the wavelength, are fully determined by the geometry of the magnetic field in the emission region.

To measure magnetic fields in the vicinity of supermassive black holes, the Main (Pulkovo) Astronomical Observatory of RAS (MAO RAS) and the Special Astrophysical Observatory of RAS (SAO RAS) proposed a dedicated program of AGN observations using the 6 m BTA (Big Azimuthal Telescope) of the SAO RAS. The research group includes V L Afanasiev, N V Borisov (SAO RAS), S D Buliga, Yu N Gnedin, T M Natsvlishvili, and M Yu Piotrovich (MAO RAS). The results of these observations are presented in Section 2.

2. Results of 6 m BTA observations in the spectropolarimetric mode of the SCORPIO instrument

Spectropolarimetric observations of AGNs were carried out on the 6 m BTA telescope of the SAO RAS in 2008–2009 [5]. AGNs with known estimates of black hole masses M_{BH} were selected. Observations were carried out using the spectral camera with an optical reducer for photometric and interferometric observations (SCORPIO) installed in the primary focus of the telescope. The CCD matrix EEV42-40 with 2048×2048 pixels 12.5×13.5 μm in size was used as a detector. As a dispersing element, volume holographic phase grating VPHG550g operating in the wavelength range 3500–7200 Å from the SCORPIO package was used. The inverse linear dispersion in the photodetector plane was 1.8 Å per pixel. Five round diaphragms with a diameter of 4.5″ were used to form a pseudo-slot with a step of 9.7 arc seconds. A Savart plate mounted behind the diaphragms was used as a polarization analyzer. The central diaphragm was used to obtain object spectra in perpendicular polarization planes, and other diaphragms were used to obtain the night sky spectra. The actual spectral resolution, which was determined by a monochromatic image of the diaphragms, was 40–42 Å. The image quality in all sets of observations was better than 2″.

The method of observations and polarization reduction is described in [6]. For wavelength calibration and determination of the relative transmission of the diaphragms, an Ar–Ne–He lamp emitting a line spectrum and a quartz lamp were used. To calibrate the spectropolarimetric tract of the spectrograph, standards from survey [7] were used. The data processing and analysis were carried out by the standard method using the specialized IDL6.2 software.

Table 1. Results of observations.

Object	m_V	z	Type	Date	t_{exp}, c	P_V, %	PA_V, deg	n
PG 0007+106	15.2	0.089	Sy1	30.11.08	3000	1.02 ± 0.38	83	0.15 ± 0.25
PG 0026+129	15.3	0.142	QSO	30.11.08	3000	1.07 ± 0.28	99	-0.45 ± 0.33
PG 0049+171	16.1	0.064	Sy1.5	24.09.09	2160	1.42 ± 0.31	247	-0.28 ± 0.18
PG 0157+001	15.7	0.163	Sy1.5	01.12.08	3000	1.78 ± 0.28	17	-0.52 ± 0.28
PG 0804+761	14.7	0.100	QSO	02.12.08	3000	1.00 ± 0.38	83	0.24 ± 0.38
PG 0844+349	14.5	0.064	Sy1	29.11.08	3000	0.85 ± 0.10	243	-1.17 ± 0.17
PG 0953+414	15.3	0.234	QSO	03.12.08	3000	0.39 ± 0.12	317	0.11 ± 0.13
PG 1022+519	15.8	0.045	Sy1	30.11.08	3000	0.83 ± 0.30	259	-2.37 ± 0.45
PG 1116+215	14.4	0.177	QSO	29.11.08	3000	0.57 ± 0.12	193	-1.26 ± 0.13
PG 2112+059	15.9	0.466	QSO	29.11.08	3000	1.04 ± 0.21	258	0.45 ± 0.17
				18.08.09	3600	1.08 ± 0.20	243	0.35 ± 0.10
PG 2130+099	14.7	0.063	Sy1	30.11.08	3000	0.62 ± 0.15	53	-0.05 ± 0.32
PG 2209+184	15.9	0.070	Sy1	24.09.08	3600	0.83 ± 0.29	200	-0.75 ± 0.21
PG 2214+139	15.1	0.066	Sy1	28.11.08	3000	1.58 ± 0.18	323	-0.69 ± 0.15
PG 2233+134	16.3	0.236	QSO	29.11.08	3000	0.67 ± 0.23	253	0.28 ± 0.28
3C 390.3	15.2	0.056	Sy1	29.11.08	3000	2.09 ± 0.22	140	-0.57 ± 0.22
				17.08.09	3600	1.58 ± 0.18	146	-0.64 ± 0.07
				24.09.09	3600	1.80 ± 0.24	144	-0.58 ± 0.06

The list of observed objects and main results are presented in Table 1, which lists the name of the object, the magnitude of its nucleus in the V band (m_V), the redshift z, the AGN type, the date of observations, the exposure time t_{exp}, the mean value of the linear polarization P_V, and the positional angle of the polarization plane PA_V in the V band. The last column of Table 1 shows the exponent n in the power-law dependence $P_l(\lambda) \sim \lambda^n$ of the linear polarization degree on the wavelength. The measurement error of the positional angle was better than $2^\circ - 3^\circ$. When calculating the exponent n by the least square method, the polarization in the emission lines was not taken into account. The obtained values of n are used below to fit a power-law radial dependence of the magnetic field in the accretion disk.

It is interesting to compare the obtained values of the polarization in the continuum and the exponent n with the black hole parameters. The analysis of data shown in Table 1 reveals an appreciable correlation between the exponent n and the black hole mass (Figs 1, 2).

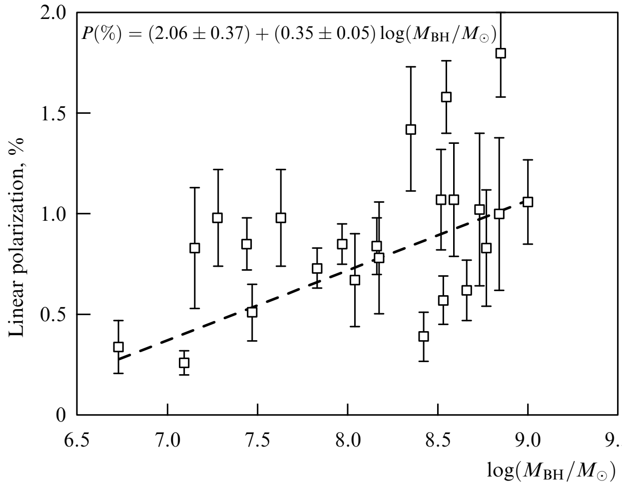

Figure 1. The dependence of the linear polarization degree on the black hole mass according to the data in Table 1.

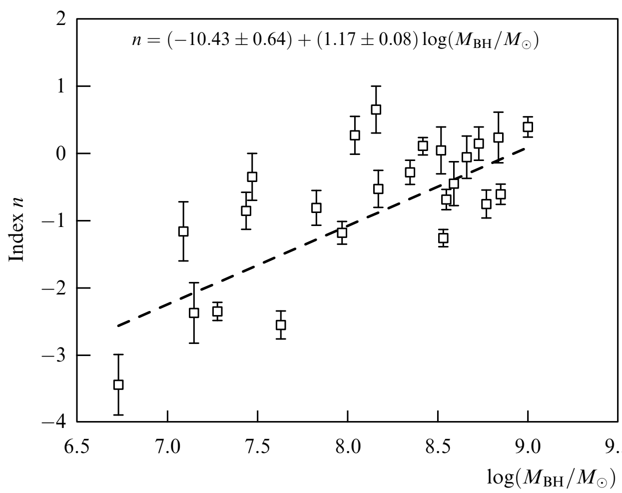

Figure 2. The exponent n of the power-law dependence of polarization on the wavelength as a function of the SMBH mass in Table 1.

3. Determination of supermassive black hole spins in active galactic nuclei

The spin and mass of a supermassive black hole are its fundamental parameters. The spin is typically described by the dimensionless parameter $a = cJ/GM_{BH}^2$, where J is the angular momentum of the black hole. The spin of a black hole varies in the range $0 < a < 0.998$ [8]. Positive spins with $a > 0$ mean that the sense of rotation of the black hole coincides with that of matter in a Keplerian accretion disk. In the case of retrograde rotation, $a < 0$.

As early as the pioneering work by Penrose [9] and Blandford and Znajek [10], it was shown that spin plays a major role in the process of energy release around a supermassive black hole. For example, the black hole spin is the key parameter in the launch of a relativistic jet due to extraction of rotational energy of the black hole via the magnetic field.

That is why direct measurement of the spin of SMBHs residing in the center of AGNs and quasars is the key problem of modern astrophysics. Presently, the SMBH spins are commonly estimated from the analysis of profiles of FeK_α lines [11–14]. For example, in papers [13–15], a detailed analysis of X-ray spectra of several AGNs detected by the

Suzaku and XMM-Newton (X-ray Multi-Mirror Mission) space observatories was carried out. Detailed profiles of FeK_α lines were obtained using the Laor, Kerr-disk, and Kerrcony software packages. As a result, papers [13, 14] reported strong bounds on spins of some AGNs. A similar analysis was also carried out for several AGNs in [16]. Nevertheless, there are substantial errors in the SMBH spin determination by different methods of processing FeK_α line profiles (see Table 6–9 in [13]). According to [13], the iron line profile in Ark 120 obtained by the Reflionx method suggests $a < 0.94$, while other variants of the same method yield $a > 0.97$ and $a < 0.87$. Interestingly, quite a different bound on the SMBH spin in Ark 120 is reported in [17]: $a \geqslant 0$.

It would therefore be useful to derive a bound for the SMBH spin using an independent method. The simplest and the most effective method is based on the estimate of the jet kinetic power, which strongly depends on the spin [18]. Here, the magnetic field generated near the SMBH horizon plays the key role.

The relativistic jet kinetic power is usually estimated from the magnetic field near the SMBH horizon (if the Blandford–Znajek mechanism [10] is involved) or at the radius of the last marginally stable orbit in the accretion disk [18, 19]. Frequently, the Eddington value of the magnetic field is assumed, implying that the energy density of the magnetic field is comparable with the total energy density of the accreting plasma generating the Eddington luminosity [1]. Exactly this estimate was used in [18].

In this paper, to estimate the SMBH spin, we use an indirect method of magnetic field determination proposed in [2–4, 19]. The method uses spectropolarimetric observations, with the Faraday rotation of the polarization plane over one free path of a photon in the process of scattering on plasma electrons taken into account. We use the data of spectroplarimetric observations of AGNs carried out with the 6 m BTA telescope [5].

According to [18], the SMBH spin can be represented in the form

$$a = \eta \left(\frac{L_{\mathrm{j}}}{10^{44}} \right)^{0.5} \frac{10^4}{B_{\mathrm{h}}} \, \frac{10^8 M_\odot}{M_{\mathrm{BH}}} \,, \tag{1}$$

where L_{j} is the kinetic power of the relativistic jet, B_{h} is the poloidal magnetic field in the SMBH ergosphere, and M_{BH} is the SMBH mass. The coefficient η depends on the physical mechanism of jet launching. In the Blandford–Znajek model [10], $\eta = \sqrt{5}$, and for Meier's hybrid model [20], $\eta = (1.05)^{-1/2}$.

To estimate the relativistic jet power, we can use the relation from [21]

$$\log \frac{L_{\mathrm{j}}}{M_{\mathrm{BH}}/M_\odot} = (38.3 \pm 0.1) + (0.55 \pm 0.06) \log \frac{L_{\mathrm{bol}}}{L_{\mathrm{Edd}}} \,, \tag{2}$$

where L_{bol} is the bolometric luminosity of the AGN and $L_{\mathrm{Edd}} = 1.3 \times 10^{46} M_8$ is the Eddington luminosity, with $M_8 = M_{\mathrm{BH}}/10^8 M_\odot$.

Of great importance is the relation between the magnetic field at the SMBH horizon B_{h} and at the radius of the last marginally stable orbit in the accretion disk B_{in}. Such a relation was found quite recently [22]: $B_{\mathrm{h}} = \chi(a)\, B_{\mathrm{in}}$, where the coefficient $\chi(a)$, depending on the BH spin, is plotted in Fig. 7 in [22].

It is also important that the magnetic field in the last marginally stable orbit B_{in} can be determined from spectropolarimetric observations [5] using the method developed in [2, 4, 19]. As a result, it is possible to determine the magnetic field strength in the region of generation of polarized radiation and then to calculate its value at the last marginally stable orbit using the most effective model of the accretion disk. According to the papers cite above, the polarization of radiation, for example, in the broad emission line region R_{BLR} is connected with the magnetic field strength B_{BLR} in this region, with Farady's rotation of the polarization plane over one free path of a photon in magnetoactive plasma in the process of scattering on electrons taken into account, as follows:

$$B(R_{\mathrm{BLR}}) = \frac{1}{0.8\lambda_{\mathrm{BLR}}^2 \sqrt{1-\mu^2}} \left[\left(\frac{P_{\mathrm{l}}(\mu)}{P_{\mathrm{l}}(\mathrm{obs})} \right)^2 - 1 \right]^{1/2} . \tag{3}$$

Here, λ_{BLR} corresponds to the wavelength of a broad emission line, for example, H_α; $\mu = \cos i$, where i is the accretion disk inclination; $P_{\mathrm{l}}(\mu)$ is the standard degree of polarization of radiation from an optically thick parallel layer with scattering seen at the angle i to the line of sight [23, 24]; and $P_{\mathrm{l}}(\mathrm{obs})$ is the observed degree of polarization, which is typically much smaller than the standard value due to Faraday's depolarization [4, 19]. The values of $P_{\mathrm{l}}(\mathrm{obs})$ found for some AGNs are presented in [5].

It is also important to determine the radial magnetic field distribution in the accretion disk, in particular, in the broad emission line region. As shown in [25, 26], first, the vertical magnetic field component is typically small and, second, a toroidal distribution of the magnetic field inside the accretion disk is most probable. It is the differential rotation of the disk that helps increase the azimuthal magnetic field component and transform the poloidal field into the toroidal one. This allows using the expression

$$B(R) = B_{\mathrm{in}} \left(\frac{R_{\mathrm{in}}}{R} \right)^n , \quad n = 1 \,, \tag{4}$$

for the magnetic field distribution inside the accretion disk. Formulas (1)–(4) allow estimating the SMBH spin from spectropolarimetric observations. The dependence of the inner accretion disk radius on the SMBH spin can be found in the literature (see, e.g., [27]).

Substituting Eqns (2)–(4) in (1) allows determining the functions

$$f(a) = \frac{\chi(a)\, a}{q(a)} \,, \quad R_{\mathrm{in}}(a) = \frac{GM_{\mathrm{BH}}}{c^2} \tag{5}$$

directly from observations. Next, by solving Eqn (5) for a, we can estimate the black-hole spin. The function $\chi(a)$ can be found in [22] and $q(a)$ in [27]. As a result, we obtain

$$a = \eta \, \frac{l_{\mathrm{E}}^{1/4}}{M_8^{1/2}} \, \frac{1}{\chi(a)} \, \frac{10^5 G}{B_{\mathrm{in}}} \,, \tag{6}$$

where $l_{\mathrm{E}} = L_{\mathrm{bol}}/L_{\mathrm{Edd}}$.

The magnetic field B_{in} can be derived from spectropolarimetric observations using Eqns (3) and (4). Because the data presented in [5] suggest that the degree of polarization does not depend on frequency, we believe that the observed value $P_{\mathrm{l}}(\nu) = 1.02\%$ also corresponds to the broad emission line

Table 2. Bounds on the SMBH spin in AGNs studied by us.

Object (number PG)	a	$B_{\rm in}$, G	$B_{\rm h}$, G
0007 + 106	0.850 – 0.920	$(5.4-9.4)\times10^3$	$(3.0-5.9)\times10^4$
0049 + 171	0.920 – 0.998	$(5.3-6.7)\times10^3$	$(3.4-6.7)\times10^4$
0157 + 001	0.830 – 0.998	$(3.7-8.0)\times10^4$	$(1.2-5.9)\times10^5$
0026 + 129	0.750 – 0.930	$(1.0-1.6)\times10^4$	$(4.50-9.95)\times10^5$
0804 + 761	0.660 – 0.830	$(0.9-1.2)\times10^4$	$(3.2-6.2)\times10^4$
0844 + 349	0.400 – 0.998	$(1.3-3.8)\times10^5$	$(0.39-1.90)\times10^6$
0953 + 414	0.600 – 0.960	$(0.50-1.65)\times10^5$	$(1.65-9.70)\times10^5$
1022 + 519	0.650 – 0.830	$(0.8-1.1)\times10^5$	$(2.9-6.0)\times10^5$
1116 + 215	0.600 – 0.750	$(2.8-3.5)\times10^4$	$(0.84-1.56)\times10^5$
2112 + 059	0.850 – 0.930	$(1.20-1.45)\times10^4$	$(6.4-9.3)\times10^4$
2130 + 099	0.550 – 0.650	$(1.7-1.9)\times10^4$	$(5-7)\times10^4$
2209 + 184	0.800 – 0.950	$(4.5-6.4)\times10^3$	$(2.3-4.2)\times10^4$
2214 + 139	0.850 – 0.985	$(0.9-1.5)\times10^4$	$(0.5-1.0)\times10^5$
2233 + 134	0.610 – 0.850	$(5-8)\times10^4$	$(1.8-4.2)\times10^5$

region, i.e., $P_{\rm l}({\rm obs}) = 1.02\%$. If we assume that $i = 60^\circ$, then $P_{\rm l}(\mu) = 2.2522\%$ [24]. As a result, Eqns (3)–(5) and (7) yield an estimate of the SMBH spin in the nucleus of PG 0007 + 106: $0.85 \leqslant a \leqslant 0.92$. The upper bound corresponds to the Blandford–Znajek process [10] with $\eta = \sqrt{5}$, and the lower bound corresponds to Meier's hybrid model [20] with $\eta = 1$.

Using the above scheme, we determined SMBH spins in AGNs from spectropolarimetric observations carried out with the 6 m BTA telescope [5] using the SCORPIO focal reducer in the spectropolarimetric mode [6]. The data were processed and analyzed using standard methods and specialized programs. The list of observed objects and the main results are presented in Table 1 in [5].

Of course, the spin estimate strongly depends, according to (6), on the magnetic field at the last marginally stable orbit of the accretion disk, which in turn depends on the inclination angle of the disk to the line of sight. For some objects studied in [5], such as PG 1057 + 001, PG 0844 + 349, PG 0953 + 414, and PG 1116 + 215, the inclination angles were determined in [28]. Interestingly, within measurement errors, the inclination angle is found to be quite large for all these objects, $i \geqslant 60^\circ$. In our calculations, we used inclination angles from [28]. We also note that for almost all objects from the Palomar–Green (PG) catalog, the inclination angle determined in [28] is close to $i = 60^\circ$. We have adopted this value for other objects from our list, which were absent in [28].

The lower bounds on the SMBH spins for the AGNs studied by us are presented in Table 2. These results suggest that spins of objects from [5] are below 0.998, which corresponds to the limit value of the spin of a stable Kerr black hole, and are always larger than 0.4.

Table 2 also presents the corresponding magnetic fields at the last marginally stable orbit in the accretion disk $B_{\rm in}$ and at the SMBH horizon $B_{\rm h}$. The transition from $B_{\rm in}$ to $B_{\rm h}$ is made using the results in [27] (see Fig. 7 in [22]).

4. Conclusion

Using the data of spectropolarimetric observations of active galactic nuclei carried out with the 6 m BTA telescope, we have estimated the spins of supermassive black holes in the centers of these galaxies. To obtain the estimates, we have used both the spectropolarimetric data and the kinetic power of relativistic jets in theses AGNs. A substantial new result found from these estimates is the value of the magnetic field at the last marginally stable orbit of the accretion disk and at the SMBH horizon.

The proposed method significantly completes the commonly used method of SMBH spin determination from the analysis of the iron line spectral shape in the X-ray spectrum of AGNs.

The present study was supported by the Program of the Presidium of the RAS No. 21, 'Nonstationary phenomena in objects in the Universe', by the Program of the Department of Physical Sciences of the RAS No. 17, 'Active processes in galaxies and extragalactic objects', and a grant from the President of the Russian Federation, 'Leading Scientific Schools', NSh-1625.2012.2.

References

1. Beskin V S *Phys. Usp.* **53** 1199 (2010) [*Usp. Fiz. Nauk* **180** 1241 (2010)]
2. Gnedin Yu N, Silant'ev N A *Astrophys. Space Sci.* **102** 375 (1984)
3. Dolginov A Z, Gnedin Yu N, Silant'ev N A *Propagation and Polarization of Radiation in Cosmic Media* (Amsterdam: Gordon and Breach Publ., 1995) [Translated from Russian: *Rasprostranenie i Polyarizatsiya Izlucheniya v Kosmicheskoi Srede* (Moscow: Nauka, 1979)]
4. Gnedin Yu N, Silant'ev N A *Astrophys. Space Phys. Rev.* **10** (1) 1 (1997)
5. Afanasiev V L et al. *Astron. Lett.* **37** 302 (2011) [*Pis'ma Astron. Zh.* **37** 333 (2011)]
6 Afanasiev V L, Moiseev A V *Astron. Lett.* **31** 194 (2005) [*Pis'ma Astron. Zh.* **31** 214 (2005)]

7. Turnshek D A et al. *Astron. J.* **99** 1243 (1990)
8. Thorne K S *Astrophys. J.* **191** 507 (1974)
9. Penrose R *Riv. Nuovo Cimento* (1) 252 (1969), Numero Speziale
10. Blandford R D, Znajek R L *Mon. Not. R. Astron. Soc.* **179** 433 (1977)
11. Fabian A C et al. *Mon. Not. R. Astron. Soc.* **238** 729 (1989)
12. Laor A *Astrophys. J.* **376** 90 (1991)
13. Patrick A R et al. *Mon. Not. R. Astron. Soc.* **411** 2353 (2011)
14. Patrick A R et al. *Mon. Not. R. Astron. Soc.* **416** 2725 (2011)
15. Brenneman L W, Reynolds C S *Astrophys. J.* **702** 1367 (2009)
16. Brenneman L W et al. *Astrophys. J.* **736** 103 (2011)
17. de La Calle Pérez I et al. *Astron. Astrophys.* **524** A50 (2010)
18. Daly R A *Mon. Not. R. Astron. Soc.* **414** 1253 (2011)
19. Silant'ev N A et al. *Astron. Astrophys.* **507** 171 (2009)
20. Meier D L *Astrophys. J.* **522** 753 (1999)
21. Foschini L *Int. J. Mod. Phys. Conf. Ser.* **08** 172 (2012); arXiv: 1107.2785
22. Garofalo D *Astrophys. J.* **699** 400 (2009)
23. Sobolev V V *Uchen. Zap. Leningr. Gos. Univ.* **116** 1 (1949)
24. Chandrasekhar S *Radiative Transfer* (Oxford: Clarendon Press, 1950)
25. Mayer M, Pringle J E *Mon. Not. R. Astron. Soc.* **368** 379 (2006)
26. Bonanno A, Urpin V *Astron. Astrophys.* **473** 701 (2007)
27. Novikov I D, Thorne K S, in *Black Holes* (Eds C DeWitt, B C DeWitt) (New York: Gordon and Breach, 1973) p. 343
28. Crummy J et al. *Mon. Not. R. Astron. Soc.* **365** 1067 (2006)

PACS numbers: 97.10.Bt, 97.80.Jp, 98.70.Qy
DOI: 10.3367/UFNe.0183.201307g.0752

X-ray binaries and star formation

M R Gilfanov

1. Introduction

Progress in X-ray astronomy gave rise to a new method for estimating the star formation rate in distant galaxies using the measurement of their X-ray emission [1, 2]. X-ray observations of nearby galaxies demonstrated that if a galaxy does not show activity from the nucleus (i.e., if the rate of gas accretion onto the central supermassive black hole is low), its X-ray radiation is mainly due to X-ray binaries. Studies of high-mass X-ray binaries in our Galaxy and in nearby galaxies by the X-ray observatories Chandra, XMM-Newton (X-ray Multi-Mirror Misson), INTEGRAL (INTErnational Gamma-Ray Astrophysics Laboratory), and ASCA (Advanced Satellite for Cosmology and Astrophysics), by the Kvant module of the 'Mir' Space Station, etc., have allowed finding the dependence of the number of X-ray binaries on the star formation rate of young stars in these galaxies.

It is well known that neutron stars and black holes are end products of the evolution of stars with masses exceeding $\approx (8-10)\,M_\odot$ (see, e.g., [3, 4]). Accretion onto these compact objects leads to an energy release comparable to their rest mass energy per unit mass of accreting gas, i.e., $L_{\rm X} = \eta\,\dot{M}c^2$, with the efficiency $\eta \sim 0.1-0.2$. If these objects are in binary systems, and the secondary star (typically, a main-sequence star, a subgiant, or a giant) either fills its Roche lobe or intensively loses mass via powerful stellar wind, the accretion of matter from the secondary leads to the appearance of a bright compact X-ray source — an X-ray binary. X-ray binaries are usually subdivided into two classes according to the mass of the donor star: high-mass X-ray binaries (HMXBs) and low-mass X-ray binaries (LMXBs). These two classes are separated by the poorly populated region from $\sim 1\,M_\odot$ to $\sim 5\,M_\odot$, in which there are virtually no bright stationary X-ray sources. The difference in the donor star mass determines the difference in the characteristic time scales of these systems. In the case of massive donors, the longest time scale, which is determined by the nuclear evolution of the star, does not exceed several dozen million years [3]. This scale is comparable with the characteristic duration of a star-formation episode; therefore, it is natural to expect that the number of such systems in a galaxy is proportional to the star formation rate (SFR) [1, 2, 5]:

$$N_{\rm HMXB}\,,\ L_{\rm X,\,HMXB} \propto {\rm SFR}\,. \qquad (1)$$

The evolution of low-mass stars, by contrast, is determined by the rate of loss of orbital angular momentum or the nuclear evolution time scale of the low-mass star, which is usually $\sim 1-10$ billion years [4]. Therefore, it is expected that the number of such systems in a galaxy is determined by the total mass of stars in the galaxy:

$$N_{\rm LMXB}\,,\ L_{\rm X,\,LMXB} \propto M_*\,. \qquad (2)$$

Classical methods of estimation of the star formation rate in a galaxy are based on measurements of the total emission from massive stars. Due to a relatively short lifetime, the number of massive stars in a galaxy can characterize the star formation rate. The radiation from massive stars can be directly measured in the ultraviolet band or by the effect of its interaction with the surrounding interstellar medium, for example, using infrared emission from dust or $\rm H_\alpha$ emission of hydrogen ionized by the ultraviolet emission of massive stars. The link between the luminosity of this radiation and the formation rate of massive stars is determined theoretically using models of population synthesis of stellar evolution (see review [7]).

The need to take corrections due to interstellar absorption into account is a major difficulty of traditional methods. Uncertainties in the parameters of the interstellar medium, its optical depth, and its dust content make the estimation of the fraction of the primary ultraviolet radiation transformed into infrared emission highly uncertain; in particular, this fraction can depend on the type of galaxy and its specific star formation rate. Another difficulty is due to the cosmological redshift, which shifts the emission frequency outside the convenient optical bands; this hampers the application of classical methods to studies of distant galaxies with high redshifts. Therefore, the appearance of a new method, which is based on the X-ray emission of accreting neutron stars and black holes, is important for testing and calibrating traditional methods, as well as for broadening their area of application.

An important feature of the new method is its weaker dependence on the interstellar absorption. Indeed, attenuating a 3 keV emission twofold requires the hydrogen column density (the hydrogen density integrated along the line of

M R Gilfanov Space Research Institute, Russian Academy of Sciences, Moscow, Russian Federation
E-mail: gilfanov@iki.rssi.ru

Uspekhi Fizicheskikh Nauk **183** (7) 752 – 761 (2013)
DOI: 10.3367/UFNr.0183.201307g.0752
Translated by K A Postnov; edited by A M Semikhatov